Surface plastic flow of three-dimensional printed polylactic acid in the tribological study of surface patterned polymer

OPEN ACCESS
IOP Publishing
Measurement Science and Technology
Meas. Sci. Technol. **33** (2022) 024001 (11pp)
https://doi.org/10.1088/1361-6501/ac3549

Surface plastic flow of three-dimensional printed polylactic acid in the tribological study of surface patterned polymer

M Ando[1], M Birosz[1], G S Gehlen[2], P D Neis[2], N F Ferreira[2] and J Sukumaran[3]

[1] Savaria Institute of Technology, Eötvös Loránd University, Budapest, Hungary
[2] Federal University of Rio Grande do Sul, Laboratory of Tribology, Porto Alegre, Brazil
[3] Laboratory Soete, Gent University, Gent, Belgium

E-mail: birosz.marton@gmail.com

Received 5 July 2021, revised 22 October 2021
Accepted for publication 1 November 2021
Published 8 December 2021

Abstract

The potential of three-dimensional (3D) printing in polymer tribology is poorly explored. Material alignment and composition play vital roles in altering the friction and wear characteristics of 3D printed materials. In the current study, 3D patterns made by fused deposition modelling are used to print advanced tribo-composites. Two different surface patterns (line and circular) are provided through 3D printing using white and silver polylactic acid (PLA). The deformation and distribution of white and silver PLA over the samples surface are observed after a wear test. Results showed that the coefficient of friction is not influenced by changes in the surface pattern. However, the wear rate increased for samples with line patterns on the contact surface, since plastic flow was more significant in this case. Moreover, the filling factor exhibited an influence on increasing the plastic flow of the contact surface for samples with a line pattern.

Keywords: 3D printing, surface pattern, polymer tribology

(Some figures may appear in colour only in the online journal)

1. Introduction

In the past few decades, interest in polymer composites has greatly increased for several tribological applications. Tribology in polymers is a complicated topic, since friction and wear behaviour are highly influenced by the type of polymer and its additives used in the tribo-system. The main advantage of using a polymer is its potential for formation of a transfer film (TF) on the counterface. A TF provides a protective layer to a hard counterface, preventing severe damage to the soft polymer as well as helping to stabilize the coefficient of friction (CoF). This protective layer acts by covering the hard asperities of the counterface [1]. However, although a TF is beneficial in some cases (protective/lubricating) it can be detrimental (due to high adhesion) in others. The process of formation and the characteristics of TFs have been previously studied by several authors [2–6]. The proper selection of additives in polymers has become a common practice for manufacturers when high wear resistance is desired in polymer tribo composites (PTCs). Other additives, such as polytetrafluoroethylene (PTFE), bronze and MoS_2, are commonly used as solid lubricants. The effect of addition on the bulk material may lead

to a reduction in the mechanical strength of the polymer composite.

The top surface of the bulk material is responsible for making contact with the counterface. For this reason, the characteristics of the top surface are related to the tribological properties of the polymer composite. In general, the additives are added to the complete bulk material rather than just to the top surface. However, some researchers (e.g. [7, 8]) have come up with solutions for adding the additives only to the top surface. Subramanian *et al* [8] fabricated what they called hybrid polymer tribo composites (hPTCs) of basalt–polyethelene with a PTFE blend on the top surface. According to the authors, the tribological performance of the hPTC matched that of commercially available PTCs used in large-scale bearing applications, with the benefit of not losing structural strength [8]. Producing PTCs using conventional technologies such as hand laying is rather well established. However, the process by itself is tedious, and very limited combinations can be made using those methods. Besides, conventional manufacturing methods do not properly place the additives in the desired locations on the PTC bulk material.

One of the recent and advanced methods for producing hPTCs is three-dimensional (3D) printing. This technique has the advantage of placing a particular material (additive) precisely in the matrix at predetermined locations. 3D printed plastics are found worldwide since they can be used in different tribological applications, ranging from domestic products to medical implants and engineering components. Besides the potential for multi-material composition, optimization of the topography and functionally graded structures are benefits of 3D printed plastic, which allows weight reduction without loss of mechanical strength [9]. There are a few 3D printing techniques that can be used for multi-material 3D printing: fused deposition modelling (FDM); selective laser sintering (SLS; solidification of powders); stereo lithography (SLA; solidification of liquid in a bath); polyjet multihole head inkjet 3D printing; and laminated object manufacturing [10–14].

So, designing a hPTC with good tribological and mechanical properties may be a challenge. Bearing this in mind, the present work offers a more comprehensive study of the tribological and surface behaviour of macro-geometrical structures (3D placed multi-materials) for 3D printed polymers. Two different surface patterns (dots and lines) and their corresponding deformation/modification after wear tests were investigated. Mechanical and tribological characteristics of the hPTC materials selected in this study are discussed throughout the paper.

2. Materials and methods

2.1. Materials

The most commonly used FDM method for 3D printing was used to print polylactic acid (PLA). In the current research, two different coloured materials (PLA extrafill traffic white and PLA silver) were used. PLA filament is made of natural ingredients and is easily biodegradable. Its material density is 1.24 g cm^{-3} and its glass transition temperature is 55 °C–60 °C based on the datasheet provided by the manufacturer (Prusa Research a.s.). Nevertheless, the literature [15–18] highlights that the mechanical properties of the finished product are highly dependent on the machining parameters. In the case of the tribological test specimens, all standard test specimens (EN ISO 20753:2014 A2 test specimen, figure 1) were prepared with the same parameters. The parameters of the process were 0.4 mm diameter extruder nozzle, 0.2 mm layer thickness, 0.8 mm contour width, 100% fill and 45° raster angle with the orientation flat on the build platform, parallel to the *x*-axis.

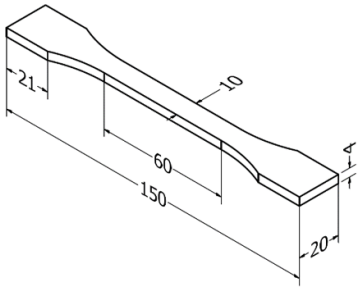

Figure 1. Tensile test specimen (ISO 527-1:2012 standard).

The tensile tests were performed using a Zwick Roell Z100 Tensile Test Machine corresponding to ISO 527-1:2012 standard (tensile speed 10 mm min^{-1}). The tensile results were evaluated using the textXpert software. The results (average of three tensile tests) were compared with the material data sheet from the manufacturer (see table 1). Since the tensile modulus could not be clearly determined on the measurement curves of the specimens, it was calculated from the slope of the line fitted to the points of the curves measured at 0.0005 and 0.0025, as recommended by the standard. However, due to the manufacturing technology, some air gaps always remain between the plastic strands, creating voids in the cross section. To calculate the tensile strength, the nominal cross section was used, as the rate of these gaps is relatively small.

2.2. 3D printing

For the production of the test specimens, a Prusa i3 MK2S printer (Prusa Research a.s.; figure 2) was used with Multi Material 2S, enabling us to use several materials at once to orient a single composite. The system is operated with a single extrusion head where the material is automatically replaced. The machine lays the required amount of the first material per layer and then unloads the filament from the extrusion head, loading the second material. Then a small amount is extracted with the wipe tower, which ensures that the residue is removed from the first material and a smooth flow is formed from the second material. A complete replacement cycle takes about 45 s. The printer always starts printing with a larger mass of material, in this case with the silver material. Later, the process

Table 1. PLA materials: mechanical properties.

Material	PLA—white			PLA—silver		
		Measured			Measured	
Data	Sheet	Mean	SD	Sheet	Mean	SD
Tensile strength (MPa)	53	48	2	51	47	2.4
Tensile modulus (MPa)	3600	2116	82	2200	2107	82

Figure 2. Prusa i3 MK2S printer used to manufacture the PLA specimens.

optimizes itself, so it can start the next layer with the material it used to finish the previous layer.

2.3. Test specimens

Cylindrical specimens with a diameter of 16 mm and a height of 24 mm were printed for the pin-on-disc tests. Two surface patterns, lines and dots, were prepared with different filling factors. It is worth mentioning that the study aims to better understand the plastic flow of the multi-material selected in this investigation, comparing its integrity when interacting with the steel counterface. This means the distribution of both silver and white PLA in the contact region will be mapped after the wear tests. This will allow us to clearly understand the plastic flow behaviour for different surface patterns.

The patterns are formed on the top, flat surface of the specimens with a depth of 3 mm. In the case of line patterns, filling factors of 25%, 50% and 75% was established. For example, a filling factor of 25% means that the white PLA covers 1/4 of the top surface, whereas the remaining 3/4 is silver PLA. The dotted surface pattern was prepared with filling factors of 25%, 37% and 50%. Pure materials were also evaluated for reference purposes, that is, specimens with only white PLA (W specimen) or silver PLA (S specimen). All specimens were rubbed against a metal disc made of SAE 1020 steel through a tribometer. A description of the test rig is provided in the next section. This disc has a diameter and thickness of 160 mm and 12 mm, respectively (figures 3(b) and (c)). A K-type thermocouple was embedded at 1.5 mm from the disc surface in order to monitor the disc temperature during the wear tests. Figure 2 shows an example of both specimens (pins), as well as a photo and a drawing of the metal disc (counterface) used in the wear tests.

Table 2 summarizes all the specimens selected in this study. In order to simplify the nomenclature of the specimens, the letters L and D are used to represent the surface patterns of lines and dots, respectively. A number along with these letters is used to identify the respective filling factor of white PLA. For instance, L25 represents the specimen with a surface of line patterns containing 25% white PLA.

Previous investigations [19–23] examined the effect of surface texture on the friction and wear of polymer materials. Those studies reported a strong influence of the type of textured surface on tribological results. By 'textured surface' those researchers defined a surface that was not smooth but which had a particular texture, or a combined form (e.g. in figure 4(a)). However, this is not the case for the specimens selected in the present study, where a surface pattern was used rather than a textured surface (e.g. in figure 4(b)).

2.4. Set-up of the wear tests

The tribological tests were performed using a pin-on-disc tribotester (UFRGS, Brazil) (figure 5). This test rig permits operation over a wide range of temperatures (up to 600 °C), sliding velocities (from 1.8 to 16 000 mm s^{-1}) and normal forces

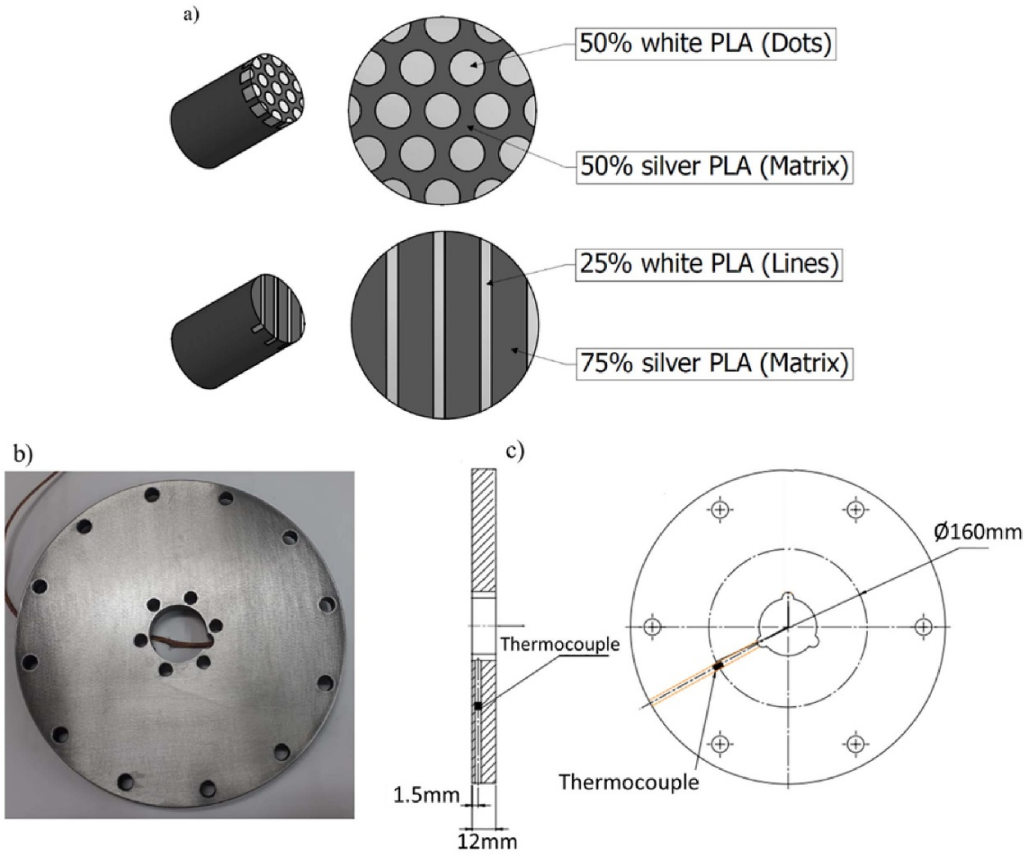

Figure 3. Specimens and counterface used in the wear tests: (a) drawing of the polymer specimens, (b) photo and (c) drawing of the SAE 1020 steel counterface.

Table 2. Formulation of the various PLA composites.

Specimen abbreviation	Pattern	White PLA (%)	Silver PLA (%)
S		0	100
W		100	0
L25	Lines	25	75
L50		50	50
L70		75	25
D25	Dots	25	75
D37		37	63
D50		50	50

(0–2500 N). Before each wear test, the surface of the steel disc was abraded in the sliding direction with sandpapers of different grit sizes (240, 300, 400, 500, 600 and 1200, in this sequence) until its surface reached a roughness Ra lower than or equal to 0.15 μm.

In the tribometer, the CoF (μ) is calculated as shown in equation (1)

$$\mu = \frac{T}{F_N R} \tag{1}$$

where T is the torque measured in the machine's shaft (N m), F_N is the normal force (N) and R is the sliding radius (m). Precision/resolution of the CoF measured by the tribotester is ±0.013, as shown in [24].

The wear tests consisted of the continuous sliding of the specimen (which works as a pin) against the steel discs. They were carried out at constant sliding velocity and normal force. The wear tests performed with each surface pattern were repeated three times. In order to avoid thermal degradation of the polymer, each test corresponded to 10 runs of 180 s each, carried out under air cooling. By doing this, the maximum bulk temperature measured beneath the surface of the counterface did not exceed 26 °C. The data acquisition sampling rate was set to 200 Hz for all tests. Table 3 summarizes the operating parameters of the wear tests.

Wear of the specimens was measured from the mass loss by subtracting the final mass of each specimen after the wear tests from the initial mass measured before wear test. An electronic balance with a precision of ±0.1 mg was used for weighing the polymer test specimens. Disc wear is not discussed in the present paper, since this metal counterpart did not show significant wear during the tests. Moreover, images of the surface of the counterface (disc) were captured using a 15 megapixel digital camera (Canon) in order to assess the formation of a polymer TF on the counterface.

Macrographs of the worn surfaces of the specimens were obtained through a stereoscope (Zeiss, model Stemi 508). Then, those macrographs were processed using a specially designed algorithm (in MatLab Mathworks®) in order to

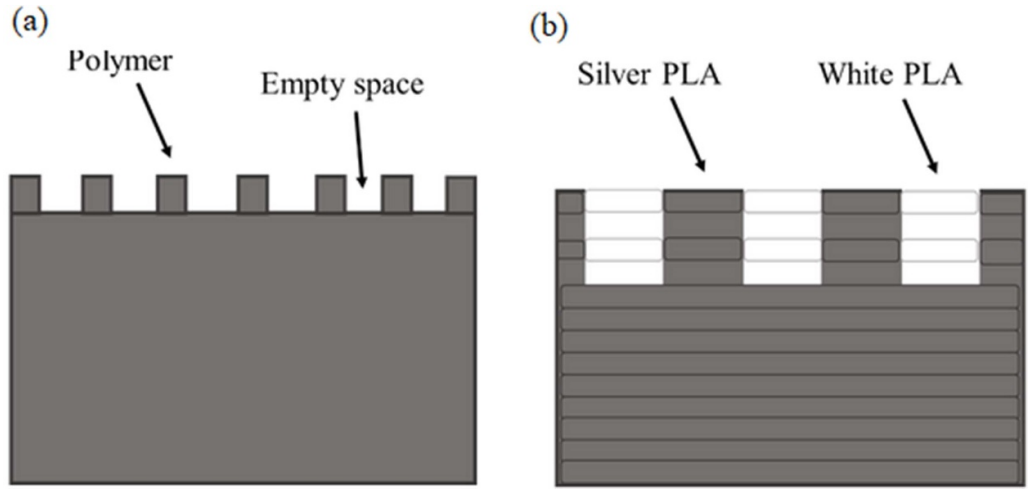

Figure 4. Types of top surfaces: (a) textured surface, alternating polymer and empty spaces (b) surface pattern, which is fully filled with polymer material, like the specimens used in the present work.

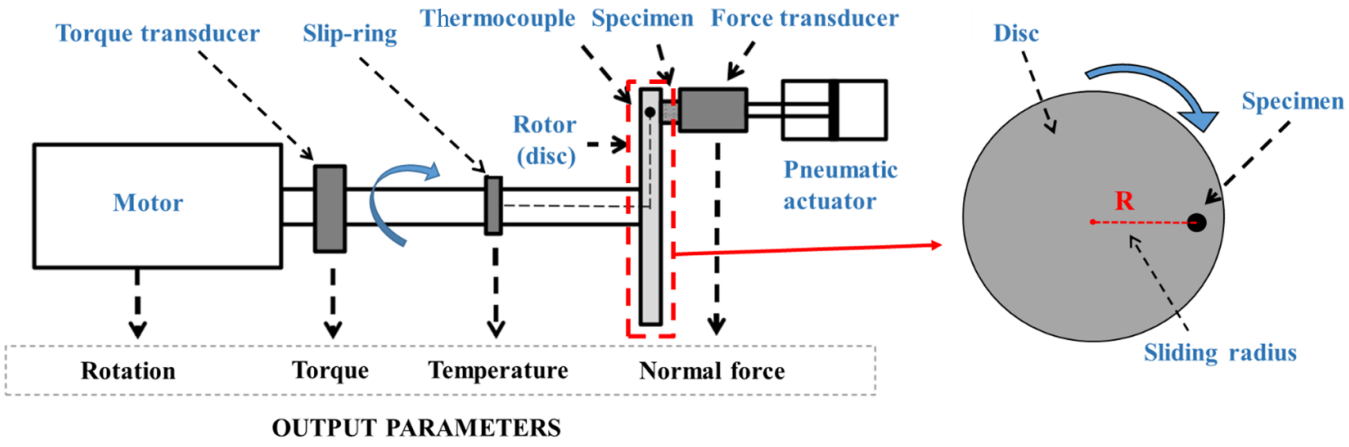

Figure 5. Scheme of the tribotester used in the wear tests.

Table 3. Contact conditions and input variables for tribological characterization.

Sliding velocity (m s^{-1})	Normal force (N)	Contact pressure (MPa)	Rotation (rpm)	Duration per run (s)	Number of runs	Total distance (m)
1.0	65	0.32	212	180	10	1800

measure the distortion (or deformation) of the specimens. The algorithm measures, pixel by pixel of the image, the portion of material which flows, displaced from its original position. The distortion was analysed for three lines in case of the specimens with a line pattern and for four dots in case of a dot pattern. The analysis was based on the area of white PLA that was displaced from its original position due to distortion (figure 6). Then, the area missing from the initial (or original) position is divided by the total area of the image (11 mm $\times$ 7 mm), providing a result that represents the fraction of the area (in %) which left the original position. This is a way to quantify the 'integrity' of the specimen, i.e. the change in geometry caused by plastic deformation.

3. Results and discussions

Figure 7 shows the average results of wear and CoF for all specimens with different surface patterns. Analysis of variance (ANOVA), with a significance level $\alpha = 0.05$, was performed to evaluate the effect of the surface pattern and the percentage of white PLA on friction and wear. CoF was relatively stable for all three repetitions (low standard deviation, expressed by the error bar). ANOVA did not show any significant difference in CoF between the specimens with different surface patterns and percentage of white PLA. For the dot pattern, the increase in the filling factor (white PLA) showed a subtle increase in friction. But this behaviour was not seen in

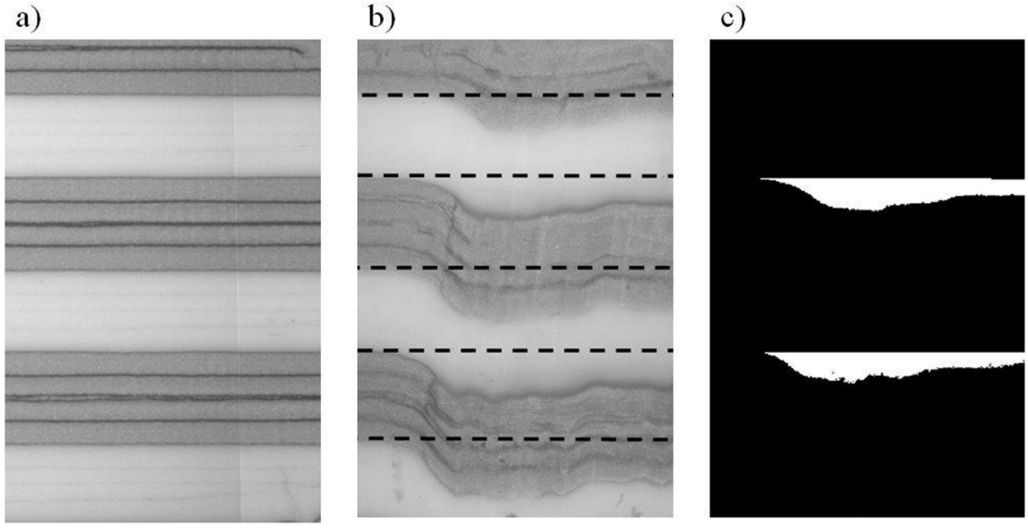

Figure 6. Example of the image processing used to assess the distortion of the specimens: (a) original surface before the tests, (b) pre-processed worn surface (specimen L50), with the position of the white PLA marked with dashed lines, and (c) binarized image showing the amount of distortion (in white).

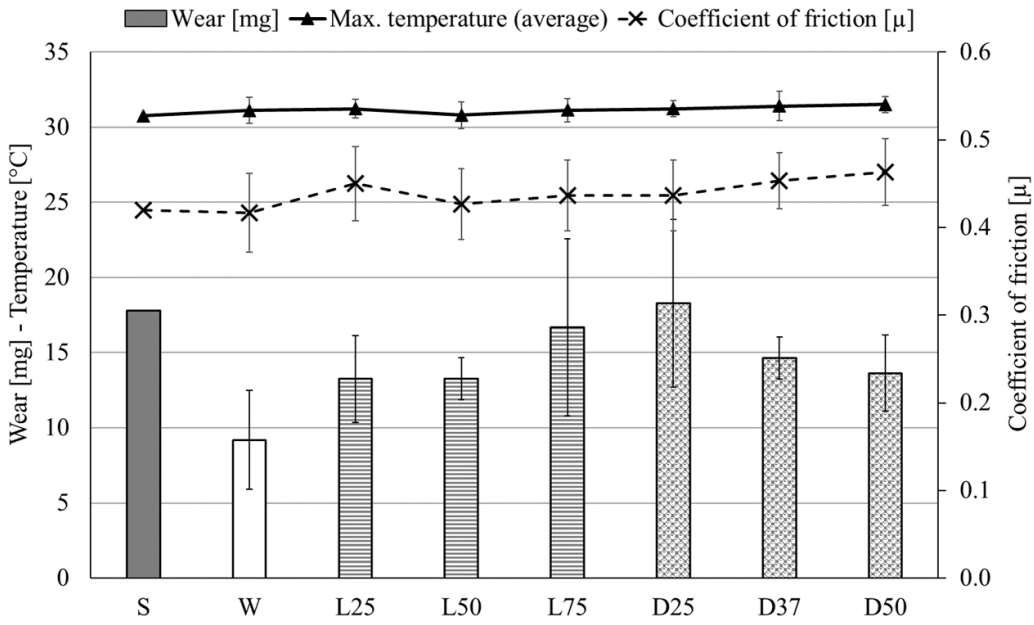

Figure 7. Results of the wear tests for all the specimens.

the line pattern specimens, where sample L25 exhibited the highest friction. As presented in table 4, the Pearson correlation coefficient seems to indicate that there is a strong correlation (1) between the mean CoF and the filling factor for the dot pattern and a weak correlation (−0.5) for the line pattern. However, the difference between the average CoF values is not significant because it is within the precision/resolution of the tribotester. Regarding wear, it was observed that wear of the pure white PLA (W) specimen is significantly lower than that of the other specimens. ANOVA also showed that there are no statistical differences in wear among all other specimens (S, L25, L50, L75, D25, D37 and D50). This means that different surface patterns caused no significant difference in wear under the applied conditions. It is noteworthy that the dynamicity involved in the TF characteristics may bring uncertainty in long-duration tests. Hence it is important to investigate the wear process to understand how this affects the integrity of the polymer material (deformation and plastic flow at the surface).

Aziz *et al* [19] examined the friction behaviour of PLA composites made by FDM with three circular surface textures (varying the diameter) through the pin-on-disc test (ASTM G-99 standard). The textures studied by those researchers were

Table 4. Pearson correlation coefficient between CoF and filling factor calculated for each type of pattern.

Specimen	White PLA (%)	Mean CoF	Pearson
L25	25	0.45	−0.50
L50	50	0.43	
L75	75	0.44	
D25	25	0.44	1.00
D37	37	0.45	
D50	50	0.46	

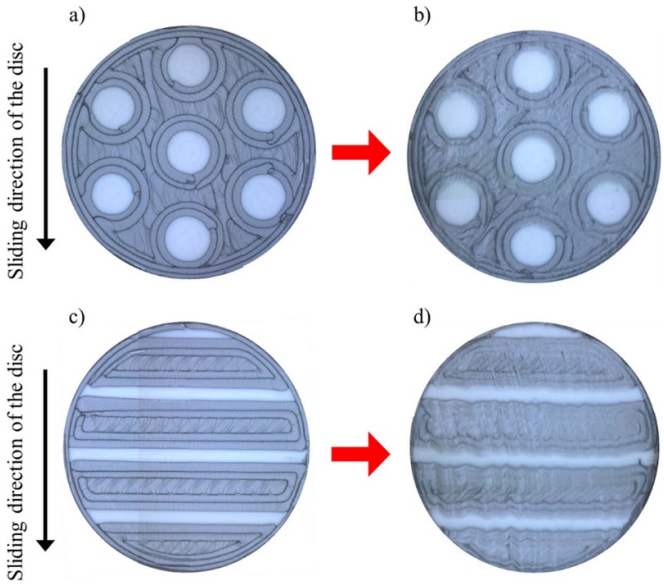

Figure 8. Macrographs of specimens D25 (above) and L25 (below): (a), (c) before and (b), (d) after the wear tests.

at a depth of 1 mm from the top surface. The authors reported different friction behaviour for the different textures with the intermediate diameter exhibiting the lowest friction. This is different from what was observed in the present study, where CoF was similar among the different surface patterns. The authors explained that the lowest friction in case of the intermediate diameter was due to the formation of a more efficient TF on the disc.

Figure 8 exhibits the surface of specimens D25 and L25 for the conditions before and after the wear tests. Overall, those surfaces represent the behaviour seen on the surface of the other specimens. There is some clear plastic deformation or plastic flow on the worn surfaces of the specimens. This can be mainly attributed to the shear force caused by the sliding condition. Considerable scratch marks or ruptured areas could not be observed. This means that abrasion was not a significant wear mechanism in the present study. The plastic flow on the polymer surface originated from a weak mechanism of adhesion. The interfacial bonding between polymer and metal was not strong enough to break the cohesive strength of the polymer, generating deformation instead of ploughing or pulling out material. Aziz *et al* [19] found that the wear of PLA composites is mainly due to adhesion and abrasion, and that there is no ploughing due to effective TF formation between the surfaces, caused by the increase in temperature.

Figure 9 presents the results of the distortion (due to plastic flow) on the surface of the polymers. Comparing the dot and line patterns, distortion appears to be prominent for the latter (line pattern). L50 exhibited the highest percentage of polymer outside the original area (5.3%). Comparatively, the highest distortion for the dot pattern was 2.5% (equally for both D25 and D50). Since the lines are perpendicular to the sliding direction, the white PLA tends to flow outside the original region when sheared. This results in a larger distortion when compared with the dotted surface (figure 10). On the other hand, dot patterns are more spread out all over the surface. For instance, specimen D50 has 19 dots of different sizes with white PLA. This makes distortion difficult and the structure of the specimen becomes more consistent. In other words, distortion is favored for line patterns since white PLA is concentrated in fewer regions (four lines). So, when a specific location on the surface begins to suffer plastic deformation, it influences the nearby regions to suffer the same effect. Also from the viewpoint of filling factor, a 50% mix provides a higher plastic flow.

Figure 11 shows the disc surface after wear tests. The formation of two different types of TF was observed for all specimens: a heterogeneously (figure 11(a)) and a homogeneously distributed film (figure 11(b)). This TF is formed due to an adhesive wear mechanism, where material from the polymer

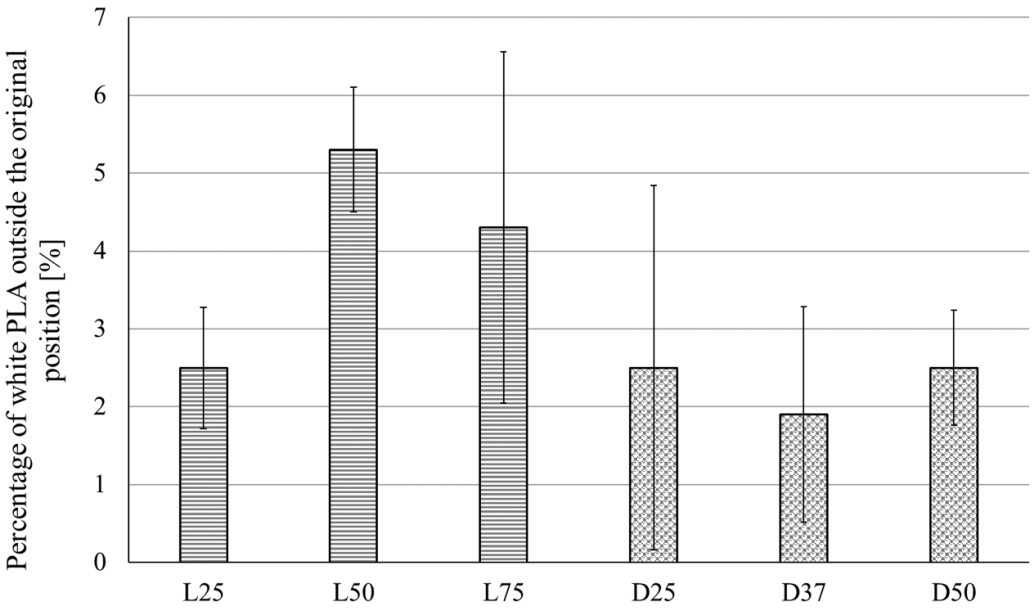

Figure 9. Results of the distortion analysis for specimens with dot and line surface patterns.

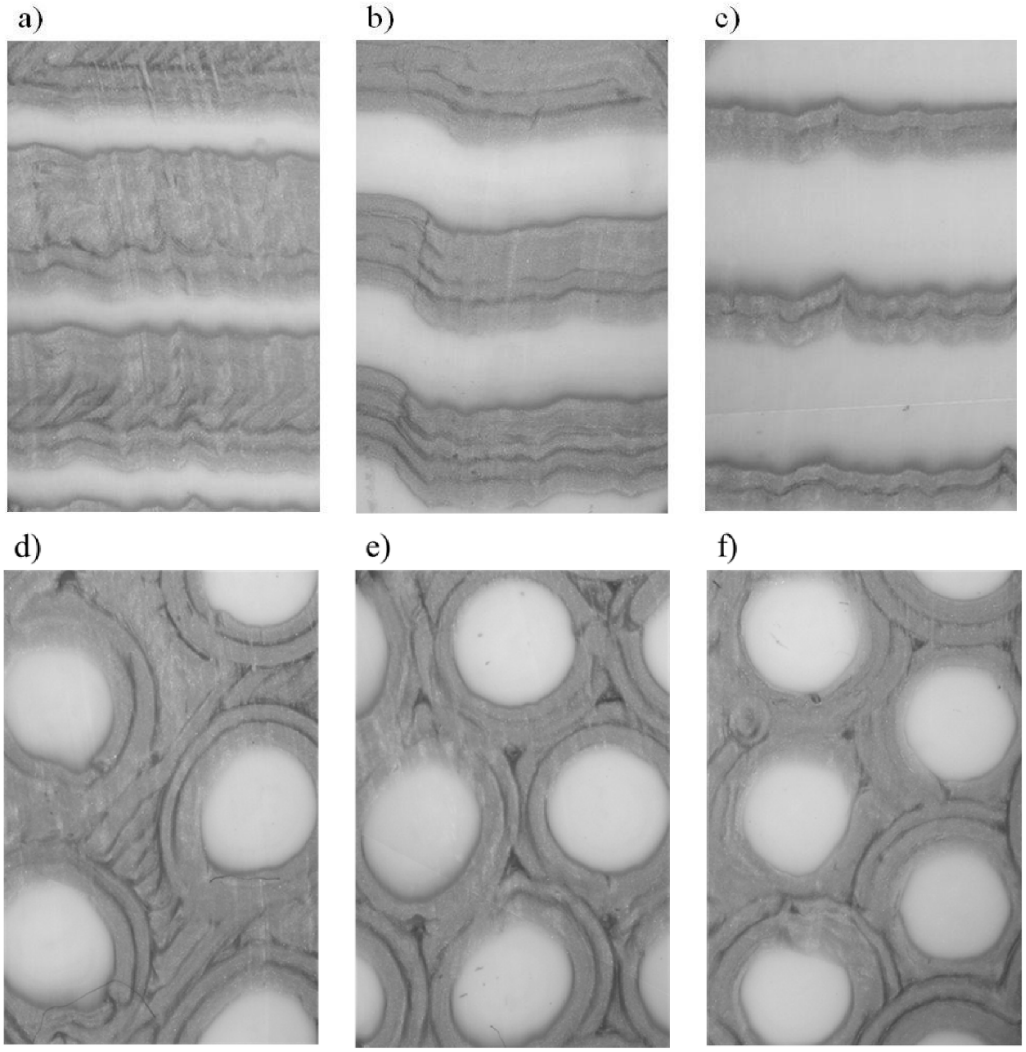

Figure 10. Worn surfaces of the specimens: (a) L25, (b) L50 and (c) L75 for the line pattern, and (d) D25, (e) D37 and (f) D50 for the dot pattern.

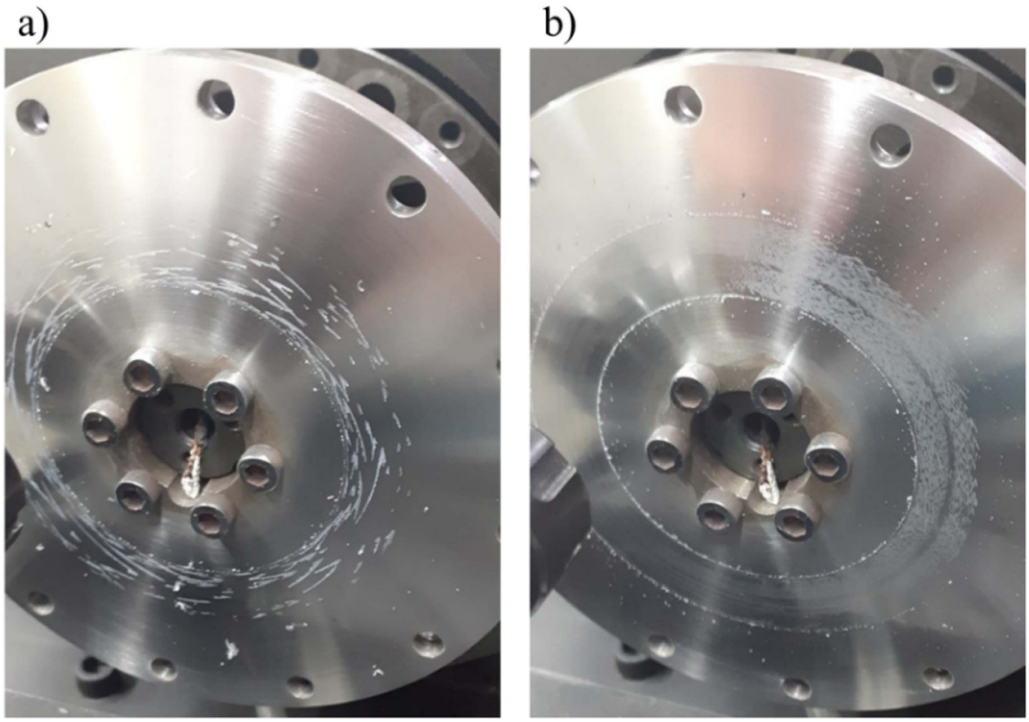

Figure 11. Images of the disc's surface showing the two different transfer films: (a) heterogeneous film, and (b) homogeneous film.

Table 5. Distribution of the transfer film on the disc surface with respect to each specimen.

Specimen abbreviation	Type of transfer film
S	Heterogeneous
W	Heterogeneous
L25	Homogeneous
L50	Homogeneous
L75	Heterogeneous
D25	Homogeneous
D37	Heterogeneous
D50	Homogeneous

is torn off from the pin and 'sticks' on the metal counterface (metal disc). The heterogeneous TF is characterized by lumps of polymer material poorly distributed on the disc surface. The homogeneous TF, on the other hand, is a more concise and well-distributed layer of polymer material on the disc surface. Table 5 shows the two typical types of TF provided by each specimen on the disc surface. No correlation was found between CoF and wear with the TF. This contradicts the research finding of Aziz *et al* [19], where the formation of a more efficient TF on the disc led to a lower CoF.

As a non-significant difference was seen in terms of mass loss for the specimens, a second test was performed with more severe conditions (normal load = 120 N, sliding velocity = 1.5 m s^{-1}). In this case, the PLA specimen suffered considerable plastic deformation, with severe damage (figure 12), in just a few runs of 180 s each. This is associated with the weak resistance of the PLA to the shear force caused by the sliding. The low shear resistance may be due to the presence of voids in the material, which is an effect commonly reported in 3D filament printing processes [25, 26]. So, on the one hand the operating parameters used in this work (see table 3) caused little wear. On the other hand, a slight increase in load and velocity caused the polymer material to suffer severe damage. It is evident that none of the specimens failed from delamination. Hence, the PLA specimens selected in this study seem to be good at preventing delamination and they rather fail due to relatively weak mechanical properties, i.e. severe damage on the surface caused by plastic flow.

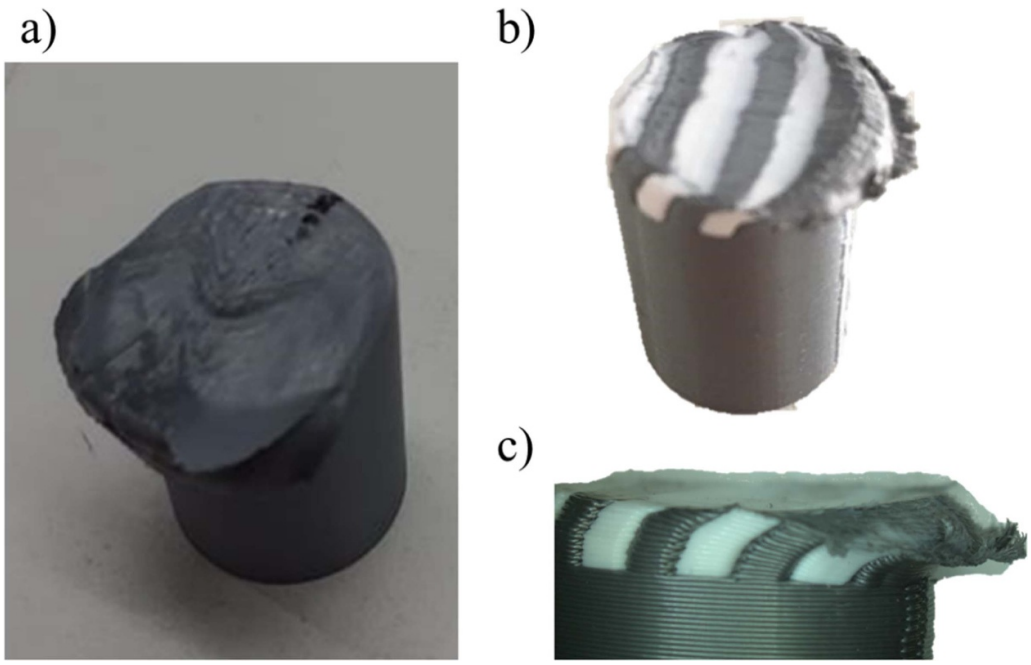

Figure 12. Images of the PLA specimens after tests with severe parameters: (a) specimen S, (b) specimen L50 whole view and (c) cross-sectional view.

4. Conclusions

The current research addresses the tribological performance of 3D printed multi-material PLA with specific surface patterns (line and dots). The following outcomes from the current study can be listed:

- Neither the line pattern nor the dot pattern made any significant difference to the tribological properties (friction and wear).
- A homogeneous TF, which is often preferred, dominated in both line and circular surface patterns. However, this was not the case for the reference materials. Hence, the pattern clearly facilitates a homogeneous TF. No correlation was seen between CoF and wear with the type of TF.
- Surface plastic flow is the preferable form of failure for all the specimens studied in the present work. Comparing the line and dot surface patterns, the latter showed more resistance to plastic flow. This occurred because dot patterns are more spread out all over the polymer surface, which makes distortion difficult and the structure of the specimen becomes more concise.

Data availability statement

The data that support the findings of this study are available upon reasonable request from the authors.

Acknowledgments

The Application Domain Specific Highly Reliable IT Solutions project has been implemented with the support provided from the National Research, Development and Innovation Fund of Hungary, financed under the Thematic Excellence Programme TKP2020-NKA-06 (National Challenges Subprogramme) funding scheme.

ORCID iDs

M Birosz https://orcid.org/0000-0002-1071-3499
G S Gehlen https://orcid.org/0000-0002-4563-7895

References

[1] Lancaster J K 1972 Polymer-based bearing materials: the role of fillers and fibre reinforcement *Tribology* 5 249–55
[2] Bahadur S 2000 The development of transfer layers and their role in polymer tribology *Wear* 245 92–99
[3] Briscoe B 1981 Wear of polymers: an essay on fundamental aspects *Tribol. Int.* 14 231–43
[4] Cho M H 2009 The role of transfer film and back transfer behavior on the tribological performance of polyoxymethylene in sliding *J. Mech. Sci. Technol.* 23 2291–8
[5] Zhang L, Qi H, Li G, Zhang G, Wang T and Wang Q 2017 Impact of reinforcing fillers' properties on transfer film structure and tribological performance of POM-based materials *Tribol. Int.* 109 58–68
[6] Ye J, Khare H S and Burris D L 2014 Quantitative characterization of solid lubricant transfer film quality *Wear* 316 133–43
[7] Subramanian K, Nagarajan R, De Baets P, Subramaniam S, Thangiah W and Sukumaran J 2016 Eco-friendly mono-layered PTFE blended polymer composites for dry sliding tribo-systems *Tribol. Int.* **102** 569–79
[8] Subramanian K, Nagarajan R, Saravanasankar S, Sukumaran J and De Baets P 2018 Dynamic mechanical and thermogravimetric analysis of PTFE blended tailor-made

textile woven basalt–vinyl ester composites *J. Ind. Text.* 47 1226–40
[9] Liu T, Guessasma S, Zhu J, Zhang W and Belhabib S 2018 Functionally graded materials from topology optimisation and stereolithography *Eur. Polym. J.* 108 199–211
[10] Sameoto D and Khondoker M A H 2017 Design and characterization of a Bi-material Co-extruder for fused deposition modeling *ASME 2016 Int. Mech. Eng. Congr. Expo. Am. Soc. Mech. Eng.* p V002T002A060
[11] Mueller J, Courty D, Spielhofer M, Spolenak R and Shea K 2017 Mechanical properties of interfaces in inkjet 3D printed single- and multi-material parts *3D Print. Addit. Manuf.* 4 193–9
[12] Bandyopadhyay A and Heer B 2018 Additive manufacturing of multi-material structures *Mater. Sci. Eng.* R 129 1–16
[13] Lopes L R, Silva A F and Carneiro O S 2018 Multi-material 3D printing: the relevance of materials affinity on the boundary interface performance *Addit. Manuf.* 23 45–52
[14] Syuhada G, Ramahdita G, Rahyussalim A J and Whulanza Y 2018 Multi-material poly(lactic acid) scaffold fabricated via fused deposition modeling and direct hydroxyapatite injection as spacers in laminoplasty *AIP Conf. Proc.* **1933** 020008
[15] Gebisa A W and Lemu H G 2019 Influence of 3D printing FDM process parameters on tensile property of ultem 9085 *Procedia Manuf.* 30 331–8
[16] Chacón J M, Caminero M A, García-Plaza E and Núñez P J 2017 Additive manufacturing of PLA structures using fused deposition modelling: effect of process parameters on mechanical properties and their optimal selection *Mater. Des.* 124 143–57
[17] Valerga A P, Batista M, Puyana R, Sambruno A, Wendt C and Marcos M 2017 Preliminary study of PLA wire colour effects on geometric characteristics of parts manufactured by FDM *Procedia Manuf.* 13 924–31
[18] Jothibabu G and Gurunathan S K 2018 Surrogate based sensitivity analysis of part strength due to process parameters in fused deposition modelling *Procedia Comput. Sci.* 133 772–8
[19] Aziz R, Haq M I and Raina A 2020 Effect of surface texturing on friction behaviour of 3D printed polylactic acid (PLA) *Polym. Test* 85 106434
[20] He B, Chen W and Wang Q J 2008 Surface texture effect on friction of a microtextured poly(dimethylsiloxane) (PDMS) *Tribol. Lett.* 31 187–97
[21] Gheisari R, Lan P and Polycarpou A A 2020 Efficacy of surface microtexturing in enhancing the tribological performance of polymeric surfaces under starved lubricated conditions *Wear* **444–445** 203162
[22] Guo Z, Xie X, Yuan C and Bai X 2019 Study on influence of micro convex textures on tribological performances of UHMWPE material under the water-lubricated conditions *Wear* 426 1327–35
[23] Cho M H and Park S 2011 Micro CNC surface texturing on polyoxymethylene (POM) and its tribological performance in lubricated sliding *Tribol. Int.* **44** 859–67
[24] Neis P D 2012 Projeto e construção de μm tribômetro com controle independente da temperatura do disco *PhD Thesis* Federal University of Rio Grande do Sul, Brazil and Ghent University, Belgium
[25] Ngo T D, Kashani A, Imbalzano G, Nguyen K T Q and Hui D 2018 Additive manufacturing (3D printing): a review of materials, methods, applications and challenges *Composites* B **143** 172–96
[26] Tronvoll S A, Welo T and Elverum C W 2018 The effects of voids on structural properties of fused deposition modelled parts: a probabilistic approach *Int. J. Adv. Manuf. Technol.* 12 3607–18